Available online at www.sciencedirect.com
SCIENCE DIRECT
ELSEVIER
Journal of Sound and Vibration 277 (2004) 669–690
JOURNAL OF SOUND AND VIBRATION
www.elsevier.com/locate/jsvi

Frequency response of pressure pulsations and source identification in a suction manifold

J.-I. Park[a], D.E. Adams[a,*], Y. Ichikawa[b], J. Bayyouk[b]

[a] School of Mechanical Engineering, Purdue University, 140 S. Intramural Drive, Ray W. Herrick Laboratories, West Lafayette, IN 47907-2031, USA
[b] Sanden International Inc., 601 South Sanden Blvd.,Wylie, TX 75098-4999, USA

Received 4 October 2002; accepted 4 September 2003

Abstract

A complicated suction manifold geometry is modelled as a simplified cylindrical annular cavity to study gas pulsations in a multi-cylinder compressor. Linear acoustic plane wave theory and a four pole parameter formulation are used to derive and solve the governing inhomogeneous equation for the forced pressure response in the manifold. By matching the lowest natural frequency of the idealized annular cavity model to that of the actual system using finite element modelling, the best possible match between the free response characteristics of the complicated and idealized manifolds is obtained. A simulation procedure for estimating gas pressure pulsations in the annular cavity connected to an anechoic inlet pipe is then described. Complicated interactions between multiple cylinder valve ports are shown to produce interesting changes in the frequency response for changes in the operating speed, and hence, the flow rate characteristics through the valves. By including a delay time for opening the valve in the mass flow rate profiles and considering the difference between the experimental and simulation results, the variable stroke of the piston and the delay times for opening the valve are estimated without solving the valve dynamic and thermodynamic equations. It is shown that the estimate of the gas pulsation in the suction manifold, which was identified using an iterative procedure, is in good agreement with the experimental result in the case of lower mass flow rate. By applying mass flow rate sinks at each valve as identified, the correlation between analytical and experimental results is shown to be much better than if the idealized, kinematically obtained source functions are used instead.

*Corresponding author. Tel.: +1-765-496-6033; fax: +1-765-494-0787.
E-mail addresses: parkjeon@ecn.purdue.edu (J.-I. Park), deadams@ecn.purdue.edu (D.E. Adams), ichikawa_yoshinobu@sanden.com (Y. Ichikawa), bayyouk@sanden.com (J. Bayyouk).

0022-460X/$ - see front matter
doi:10.1016/j.jsv.2003.09.020

1. Introduction

1.1. General

Gas pulsations are complicated in multi-cylinder compressor suction and discharge manifolds because of the interactions between different cylinder valves. The frequency response analysis and source identification of these types of interactions in a general suction manifold are the two objectives of the work discussed here. Pressure pulsations in a suction manifold are generated by the reciprocating actions of pistons including the rapid opening and closing of automatic valves. While the suction valves are open, the working compressor fluid is passed from the suction manifold into the compressor cylinder via a pressure differential that oscillates with each compression cycle for all cylinders in the compressor housing. If the pulsation levels are of sufficient amplitude, they can affect the valve opening and closing times by exciting the dynamics of the valves during the in-take process. In fact, the valve dynamics are shown to play a major role here in modulating the idealized flow profiles through each valve. Gas pulsations generally tend to degrade compressor performance and increase the overall noise levels through either airborne or structure-borne noise radiation to the surroundings. Pressure pulsations in the suction manifold may also cause backflow to occur if the amplitudes of the pressure pulsations become larger in magnitude than the pressure loss across the valve.

1.2. Description of approach

This research aims to identify the suction pressure free and forced response characteristics by implementing a set of mathematical models and a simulation procedure. After solving the linear acoustic equations that govern the gas pulsations in a simplified annular cavity model, significant factors in understanding the dynamics within a suction manifold are explored. Specifically, the two primary objectives of this research are: (1) to develop an explanation for changes in the resonant forced response behavior of a suction manifold for changes in the mass flow rate spectrum using computer simulations and (2) to estimate the modified source functions using experimental data.

Consider the first objective, to explain the frequency response sensitivity of the multi-cylinder suction manifold to changes in operating speed. In most typical applications involving noise and vibration, a change in the source/excitation does not change the natural characteristics of the system (i.e., resonant frequencies) because these characteristics are global properties of the system; however, in a multi-cylinder suction manifold the flow rates from each of the valves ‘conspire’ to modify the overall resonant behavior of the manifold even though the resonances remain unchanged. In other words, the multiple valves serve as multiple sinks, which combine to effectively change the frequencies of greatest amplification for different operating speeds.

Consider the second objective, to identify modified sources of the gas flow through each suction port. The artificial volume flow rates such as a square wave and saw-toothed wave have been used in the simulation for the gas pulsation in the past [15,17,26,27]. However, the sources are very dependent on the operating conditions and are complicated. Therefore, the source has to be identified more realistically when it is desirable to investigate the other characteristics using the flow sources. As mentioned above, pressure pulsations do alter the performance of compressors and one way in which they do that is to introduce oscillations in the ideal mass flow rates, which are based entirely on the kinematics. Once this source/excitation is estimated using an iterative inverse technique, it can be applied to the simulation model to calculate the predicted pressure pulsation using a computer simulation and then these analytical results can be compared to the experimental data. The iterative approach used to estimate the flow source profile is based on two primary assumptions. First, all valves in the multi-valve compressor are assumed to extract gas from the manifold in the same way; consequently, the profile is estimated such that when it is applied with the proper phase to each valve during a cycle, the resulting pressure pulsations in the experimental data and the analytical simulation match. Second, the natural characteristics of the annular cavity model are assumed to capture the most important dynamics of the actual manifold so that any discrepancy in the experimental and simulation pressure can be treated as an error in the excitation/source.

The first step in achieving these two objectives is to model the unsteady flows in an annular shaped suction manifold of a multi-cylinder compressor. A simplified annular passage model of average, uniform cross-sectional area is used to model a rather complicated manifold geometry. The analysis results using the simplified model provided basic insights of fundamental importance into the suction manifold gas pulsations.

1.3. Literature review

Various theoretical and experimental analyses of pressure pulsations in compressor manifolds have been discussed in the literature. Many of the most relevant articles are summarized next in order to better define the contribution of the work discussed here. The governing continuous acoustical equations for the dynamic pressure response [1] have been derived and solved in many references. For instance, Doak [2] used a one-dimensional inhomogeneous wave equation to describe mass density fluctuations in a continuous material. Also, Franken [3] analyzed the sound generated by mass or heat flow in a cylindrical cavity due to a point source. Cummings [4] discussed sound transmission in rectangular and circular sections with curved elbow bends and showed that curved bends transmit very efficiently with non-uniformity in the acoustical pressure and axial particle velocity fields due to modification of the propagation wave numbers. Subrahmanyam et al. [5] derived a family of exact solutions for quasi one-dimensional, transient acoustic wave propagation problems in ducts with mean temperature and cross-sectional area variations in the absence of mean flow.

Several researchers have also developed methods of analyzing two-dimensional acoustic dynamic pressure fields. For instance, Lai and Soedel [6] developed a general procedure for analyzing curved or flat thin two-dimensional muffler elements using Hamilton's principle to derive the dynamical system equations and four pole parameters based on modal expansion techniques to solve the equations for flat rectangular, cylindrical annular, and circular boxes. Lai and Soedel [7, 8] also went on to develop similar techniques for muffler elements of non-uniform depth and multi-component muffler systems. Kim and Soedel [9–11] developed a general procedure for deriving four pole parameters to solve for the three-dimensional pressure response using modal expansion methods in more complex acoustic systems with multiple components paying particular attention to the annular cavity with small lumped parameter cavities. Kung and Sing [12] proposed an experimental modal analysis technique for identifying model parameters in a three-dimensional acoustic cavity with damping. Pan and Jones [13] also analyzed gas pulsations for an inhomogeneous wave equation with spherical co-ordinates. Note that much of the four pole parameter approach was developed for mechanical applications by Snowdon [14].

Global models have also been used to analyze the pressure response in systems of acoustic cavities. For instance, Sun and Ren [16] simulated gas pulsations using the equations of thermodynamics, heat transfer, pulsations, and valve dynamics. Zhou and Hamilton [24] developed the simulation model for multi-cylinder reciprocating compressor considering real gas properties, heat transfer and gas leakage.

Many application-specific papers have also appeared in the literature involving the use of four pole parameters. For instance, Elson and Soedel [18] developed a mathematical model to study discharge valve responses and plenum pressure pulsations across compressor valves. Kim and Soedel [19] also studied a shell cavity connected to an anechoic pipe with a single and double input using a four pole parameter approach. Schewerzler and Hamilton [20] analyzed a three in-line compressor model taking into account the effects of pressure pulsations in the suction and discharge plenums, heat transfer from the gas on the suction and discharge sides, and the interactions of the cylinders through the common plenum. Soedel and Baum [21] analyzed a four cylinder compressor model and studied the effects of natural frequencies and modes in the resultant gas oscillations inside the manifold using a Helmholtz resonator approach. Lai et al. [22] studied the validity of the idealized shape approximations, which is suitable for a fast and qualitative understanding, by analyses of a compressor head and bullet shape muffler. Singh and Soedel [23] considered the kinematic and geometric interactions in a reciprocating compressor using an iterative procedure to account for the back pressure effect in a two cylinder high speed refrigeration compressor. Lai and Soedel [15,26] used the artificial volume flow rate assumptions such as squared waves to analyze a rectangular box type compressor head cavity. Several articles on multi-cylinder compressors are also relevant to the present study including the work by Zhou and Hamilton [24], Kim [25], and Lai and Soedel [26]. Lastly, the short course text book by Soedel [27] contains an overview of many of these previous results in addition to a summary of the techniques in Soedel's textbook on vibrations in shells and plates [28].

This paper studies the differences in free and forced response characteristics between an actual suction manifold with a complex geometry and an idealized annular cavity model. The analytical techniques used to examine these differences include modal expansion theory as well as the four pole parameter approach. Using these simulations as a tool for examining the manifold dynamics, it is shown that the multiple cylinder valves, each acting as a flow rate sink, interact to produce different resonant conditions than those that might be expected based solely on the natural modes of the manifold. It is also shown that a modified flow source profile with valve opening delay times included at each valve port should be identified in order to best correlate simulation and test results.

1.4. Engineering assumptions

The fundamental assumption used to acoustically model the manifold is that the fluid particle waves within the gas are plane waves, which are defined as waves that have the same properties at any position on the plane surface that is perpendicular to the direction of propagation of the waves. Plane waves can exist and propagate along a long straight tube or duct, for instance, under

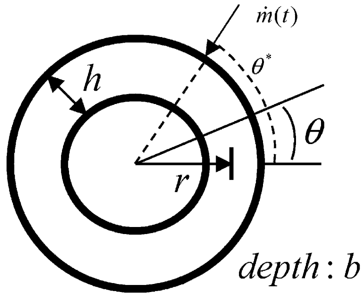

Fig. 1. Schematic of an annular cavity with a single flow source/sink.

the condition that the cross-sectional dimensions are smaller than the shortest wavelength of interest (i.e., maximum $(b, h) < \lambda$). In these circumstances, plane wave theory is valid below the frequency at which a cross-mode effect takes place. Other assumptions are the amount of fluid in the element is conserved (mass continuity), the process in the element is adiabatic (i.e., there is no flow of heat in or out of the element), the undisturbed fluid is stationary (i.e., there is no mean fluid flow), the cavity walls are infinitely rigid, the fluid is inviscid, and body forces are negligible (i.e., potential energy due to gravity is ignored). In this paper, the annular cavity shown in Fig. 1 is considered as an extension of a rectangular tube section.

The pressure variation along the radial direction in the annular cavity is not included because the length difference between the inner and outer radius is small enough to justify an assumption of uniform pressure distribution along the radial direction (i.e., plane wave assumption). Annular cavities are found in many actual products, such as hermetic reciprocating compressors, or water jackets of reactors.

1.5. Governing dynamical system equations

With these assumptions, the linear homogeneous equation describing freely propagating fluid particle waves with fluctuating pressure, $p(\theta, t)$, in an annular cavity can be expressed as [2,6,10]

$$\frac{1}{r^2}\frac{\partial^2 p}{\partial \theta^2} - \frac{1}{c^2}\frac{\partial^2 p}{\partial t^2} = 0 \tag{1}$$

and the associated natural modes, $(p_k)_i$ for $i = 1, 2$, and frequencies, ω_k, can be obtained using the separation of variables technique:

$$(p_k)_i = \sin k(\theta - \phi_i), \tag{2}$$

where for $\phi_1 = 0$, $(p_k)_1 = \sin k(\theta)$ and for $\phi_2 = \pi/2k$, $(p_k)_2 = -\cos k(\theta)$, and

$$\omega_k = k(c/r), \tag{3}$$

respectively, where c and r are the speed of sound and the mean radius of the annular cavity, respectively, and k is the integer which determines the mode of interest. Also ϕ_1 and ϕ_2 are somewhat arbitrary phase angles, which are selected to ensure that the two modes for each repeated frequency are orthogonal in the sense of

$$\int_0^{2\pi} \sin k(\theta - \phi_1)\sin k(\theta - \phi_2)\,\mathrm{d}\theta = 0. \tag{4}$$

Each value of k is associated with two spatial mode shapes with identical frequencies; i.e., each mode is a so-called repeated root. The presence of repeated roots means that the annular cavity possesses two identical frequencies for each mode whereas the actual, physical manifold possesses two slightly different (split) frequencies associated with its orthogonal modes. Also all flow sources, or sinks in the case of the valve ports, are assumed to have relatively small dimensions compared to the overall size of the cavity and to the wavelength corresponding to the highest frequency of interest; therefore, the source can be approximated as a point source as in Refs. [1, 2] using a Dirac-delta function. According to Zhow and Kim [29], the point source can be used only for one-dimensional systems due to a convergence problem. It is noted that the source for the excitation of a suction gas oscillation is generally considered to be the mass flow rate through the valves as well as the inlet. A periodic mass flow rate through the valve can either be assumed from the kinematics or can be computed from the cylinder and valve simulation models. In this paper, the flow rate is first assumed to be periodic based on the kinematics of the compressor but is then estimated using experimentally measured dynamic pressure data.

By treating the source in this way, the inhomogeneous plane wave equation of an annular cavity for the fluctuating pressure becomes

$$\frac{1}{r^2}\frac{\partial^2 p}{\partial \theta^2} - \frac{1}{c_0^2}\frac{\partial^2 p}{\partial t^2} = -\frac{\ddot{m}}{rA}\delta(\theta - \theta^*), \tag{5}$$

where $\delta(\theta - \theta^*)$and θ^* define the Dirac-delta function and the location of the point source, respectively, $\ddot{m}(t) = \partial(\dot{m}(t))/\partial t$, where $\dot{m}(t)$ is the mass flow rate (source function), and A is the constant cross-sectional area of the annular cavity [6–8,11]. The general solution of Eq. (5) is assumed to be an infinite series:

$$p(\theta, t) = \sum_{k=1}^{\infty} \eta_k(t) p_k(\theta), \tag{6}$$

where $p_k(\theta)$ are the kth natural mode components in the θ direction and $\eta_k(t)$ are the modal participation factors, which are unknown and are determined by exploiting the orthogonality property of each mode.

To solve the governing equation, the mass flow rate, $\dot{m}(t)$, is transformed into the frequency domain in terms of the volume velocity, $Q_n(n\omega)$, as follows using a complex Fourier series:

$$\dot{m}(t) = \sum_{n=-\infty}^{\infty} \rho_0 Q_n\, \mathrm{e}^{\mathrm{j}n\omega t}, \tag{7}$$

where $\rho_0 Q_n(n\omega)$ are the coefficients of the Fourier transform for the purely periodic mass flow rate. The solution for the pressure response for the single flow source input is then found to be

$$p(\theta, t) = p(\theta, t)_1 + p(\theta, t)_2 = \sum_{k=1}^{\infty}\sum_{n=-\infty}^{\infty} \frac{\mathrm{j}n\omega\rho c^2 Q_n \cos k(\theta - \theta^*)}{rAN_k[(\omega_k^2 - (n\omega)^2) + 2\mathrm{j}n\omega\omega_k\zeta_k]}\mathrm{e}^{\mathrm{j}n\omega t}, \tag{8}$$

where $p(\theta, t)_1$ and $p(\theta, t)_2$ are the fluctuating pressures for the associated natural modes.

Next, four pole parameters are used to account for the numerous sources/sinks of flow within a multi-cylinder manifold with N_v valves. Four pole parameters are very useful for the analysis of composite acoustic systems and have been widely used to analyze gas pulsations in cavities. The annular cavity can be described by four pole parameters as follows:

$$\begin{bmatrix} Q_{2n} \\ P_{2n} \end{bmatrix} = \begin{bmatrix} A_n & B_n \\ C_n & D_n \end{bmatrix} \begin{bmatrix} Q_{1n} \\ P_{1n} \end{bmatrix}, \tag{9}$$

where A_n, B_n, C_n, D_n are inverse coefficients of four pole parameters and subscripts 1, 2 indicate input (anechoic port) and output (valve port), respectively. Since the relation between the pressure at any position inside the cavity and the input/output volume flow rate at the single frequency, $n\omega$, is assumed to be given by Ref. [9–11]

$$P_n(\theta)e^{jn\omega t} = f_{1n}(\theta, n\omega)Q_1 e^{jn\omega t} - f_{2n}(\theta, n\omega)Q_2 e^{jn\omega t}. \tag{10}$$

The four pole parameters for each input/output could be obtained separately after some extensive matrix algebra. According to Snowdon [14], the inverse coefficients of the four pole parameters are defined as follows:

$$A_n = \left.\frac{P_1}{P_2}\right|_{Q_2=0} = \frac{f_{1n}(\theta_1, n\omega)}{f_{1n}(\theta_2, n\omega)}, \quad B_n = \left.\frac{Q_1}{P_2}\right|_{Q_2=0} = \frac{1}{f_{1n}(\theta_2, n\omega)},$$

$$C_n = \left.\frac{P_1}{Q_2}\right|_{P_2=0} = -f_{2n}(\theta_1, n\omega) + \frac{f_{1n}(\theta_1, n\omega)}{f_{1n}(\theta_2, n\omega)} f_{2n}(\theta_2, n\omega), \quad D_n = \left.\frac{Q_1}{Q_2}\right|_{P_2=0} = \frac{f_{2n}(\theta_2, n\omega)}{f_{1n}(\theta_2, n\omega)}.$$

For example, A_n and B_n are found to be

$$A_n = \frac{\sum_{k=1}^{\infty} \dfrac{jn\omega\rho c^2}{rbhN_k[(\omega_k^2 - (n\omega)^2) + 2jn\omega\omega_k\zeta_k]}}{\sum_{k=1}^{\infty} \dfrac{jn\omega\rho c^2 \cos(k(\theta_2 - \theta_1))}{rbhN_k[(\omega_k^2 - (n\omega)^2) + 2jn\omega\omega_k\zeta_k]}},$$

$$B_n = \frac{1}{\sum_{k=1}^{\infty} \dfrac{jn\omega\rho c^2 \cos(k(\theta_2 - \theta_1))}{rbhN_k[(\omega_k^2 - (n\omega)^2) + 2jn\omega\omega_k\zeta_k]}}$$

and C_n and D_n can be similarly obtained. After describing the anechoic boundary condition with the impedance function at the entrance of the anechoic pipe,

$$Z_{ex} = \frac{P_{1n}}{Q_{1n}} = -\frac{\rho c}{S_e}, \tag{11}$$

where S_e is the cross-sectional area of the anechoic pipe and Z_{ex} is the input impedance, the transfer function between the flow rate at the inlet and the flow rate at any given valve port can be expressed [6,10] as

$$T_{Qn}(\omega) = \frac{Q_{2n}}{Q_{1n}} = A_n + Z_{ex}B_n \tag{12}$$

and the pressure response for a single input/single output in the annular cavity is computed directly using this transfer function:

$$p(\theta,t)=\sum_{n=-\infty}^{\infty}\sum_{k=1}^{\infty}\frac{\mathrm{j}n\omega\rho c^2 Q_{2n}(n\omega)\left[\dfrac{1}{T_{Q_n}(n\omega)}\cos k(\theta-\theta_1)-\cos k(\theta-\theta_2)\right]}{rAN_k[(\omega_k^2-(n\omega)^2)+2\mathrm{j}(n\omega)\omega_k\zeta_k]}\,\mathrm{e}^{\mathrm{j}n\omega t}. \tag{13}$$

The expression above is for a single flow source only; if there are N_v valves in the compressor, then this expression must be applied N_v times separatelly and the results superimposed to obtain the total dynamic pressure as calculated in this work for $N_v = 7$. The solution to Eq. (13) is simulated for multiple valves using the procedure illustrated in Fig. 2. By assuming volume flow rates (mass flow rate over density of flow) of the form

$$Q_k=\frac{1}{N}\sum_{r=0}^{N-1}\frac{\dot{m}(r\Delta t)}{\rho}\,\mathrm{e}^{-\mathrm{j}(2\pi kr/N)}. \tag{14}$$

where N is the total number of data sampling points, $k = 0, 1, 2, \ldots, (N-1)$, and the sum denotes the discrete Fourier series of Q_k, the pulsation pressure in the linear suction manifold model is also found to be periodic with Fourier series coefficients

$$P_k=\frac{1}{N}\sum_{r=0}^{N-1}p(r\Delta t)\,\mathrm{e}^{-\mathrm{j}(2\pi kr/N)} \tag{15}$$

and is calculated from Eq. (13) using the inverse coefficient of the four pole parameters and the flow transfer functions. The pressure response at the output port excited by each input is calculated by multiplying the input volume flow rate for each compressor valve by the respective

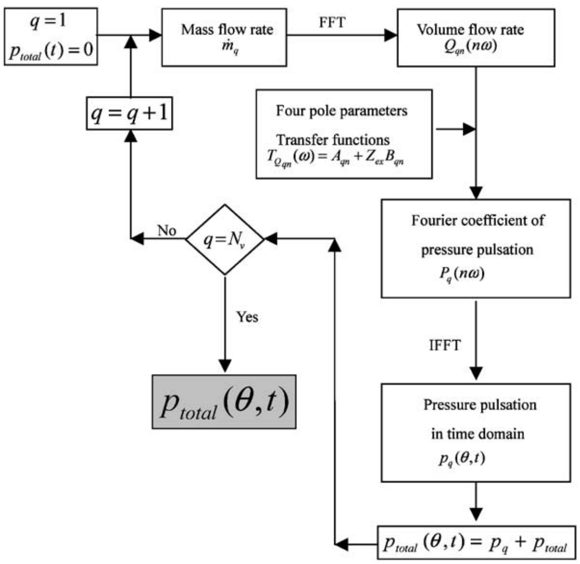

Fig. 2. Flow chart for simulation with N_v cylinders.

transfer function. The total pressure response is obtained by superimposing the responses excited by each input and then inverse Fourier transforming the frequency spectrum.

2. Analysis

2.1. Resonance conditions of the complex manifold via the finite element method

Before proceeding to discuss the results of the simulation and the various resonant conditions for different operating speeds, several parameters in the annular cavity model must be specified including the mean radius, r, of the cavity, the depth, b, and the width, h, of the cavity (where the cross-sectional area is $A = bh$), and the diameter of the anechoic inlet, D_e. If the actual manifold of interest is purely annular in nature, then choosing these parameters is trivial; however, if the annular volume is more complex as is often the case, then the parameters must be chosen carefully in order to achieve the best possible correlation between the experimental and analytical results. In particular, r is especially important because recall from Eq. (3) that the natural frequencies of the volume are determined by the quotient of r and the speed of sound in the refrigerant of interest.

Because the natural frequencies and mode shapes of a complex manifold geometry cannot be computed analytically, a two-dimensional finite element analysis is applied instead to choose r such that the idealized annular volume model has a fundamental natural frequency that falls between the two natural frequencies obtained for the complex manifold. Note that in this case, it is not possible to select r such that the model and the actual manifold have the exact same natural frequencies because the actual manifold contains asymmetries that cause the repeated roots at each mode of the axisymmetric annular manifold model to split apart. The complex manifold is modeled using two-dimensional acoustic fluid elements (fluid 29) as shown in Fig. 3. The natural

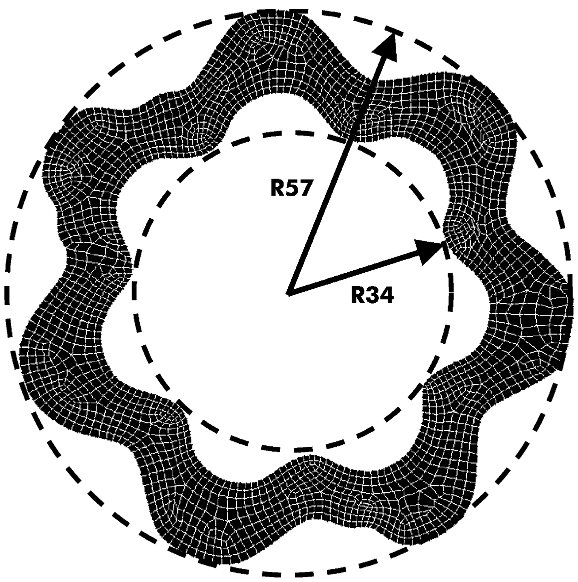

Fig. 3. Complex manifold geometry and mesh.

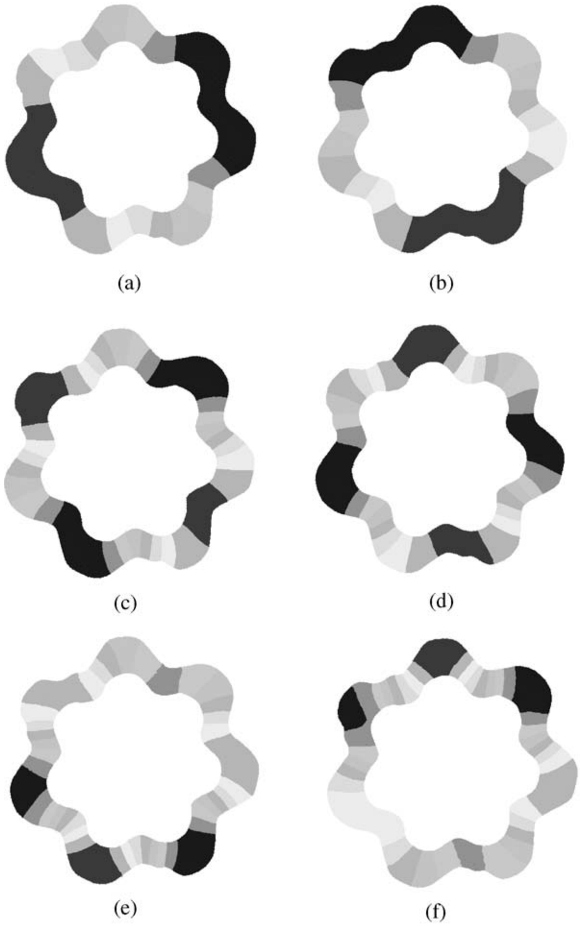

Fig. 4. Mode shapes of the complex suction manifold at natural frequencies: (a) 500 Hz, (b) 524 Hz, (c) 1010 Hz, (d) 1040 Hz, (e) 1525 Hz, and (f) 1550 Hz.

Table 1
Resonant frequencies of the complex suction manifold ($c = 160.8$ m/s)

Mode 1	ω_{R1} (Hz)	Mode 2	ω_{R2} (Hz)	Mode 3	ω_{R3} (Hz)
1	500	1	1010	1	1525
2	524	2	1040	2	1550

modes of a particular complex manifold geometry at each frequency are shown in Fig. 4. Note the "dipole type" modes, which are about 90° out of phase at two slightly different frequencies due to the asymmetric shape of the manifold. Resonant frequencies obtained in the FEA are listed in Table 1; there are two frequencies and two orthogonal shapes for each mode.

The results of the finite element analysis showed that: (1) the natural frequencies of the suction manifold depend on the mean radius, (2) the amplitude scales of the modal pressure

Table 2
Natural frequencies of the simplified suction manifold (mean radius = 50 mm, unit: Hz)

h (mm)	Mode 1 (0°)	Mode 1 (90°)	Mode 2 (0°)	Mode 2 (90°)	Mode 3 (0°)	Mode 3 (90°)
8	512	512	1023	1023	1535	1535
10	512	512	1024	1024	1535	1535
12	512	512	1024	1024	1535	1535
14	512	512	1025	1025	1535	1535

distributions in the suction manifold decrease as the length between the inner and outer radius is increased, and (3) there is no change of natural frequencies if the mean radius is the same for slightly different geometries; therefore, the simple annular cavity model used in this work is justified.

The frequency and mode shape results for the FEM of the idealized annular manifold geometry are given in Table 2 and Fig. 5 for the first three modes. In order to achieve the best match between the actual manifold frequencies and those of the annular volume, the mean radius is selected to be 50 mm, which places the first two natural frequencies directly between the first two modes of complex suction manifold.

2.2. Changes in frequency response with operating speed

The main purpose of this section is to identify the sensitivity of each pulsation frequency response at the different compressor operating speeds. According to Pan and Jones [13], it is shown in the experiment that the sound pressure level was dramatically amplified when the harmonics of the fundamental compressor operating frequency coincides with an acoustic cavity resonance. In this section, a constant amplitude sinusoidal input with the harmonics of the fundamental compressor operating frequency is used to calculate the sensitivities as shown in Fig. 7. An illustration of the procedure for obtaining the sensitivities is shown in Fig. 6. Note that only the harmonics of the operating frequency are chosen in each case because only these frequencies are likely to be found in the flow source functions at the shaft speed of interest. The chosen set of fixed manifold parameters for this example is as follows: $r = 50\,\mathrm{mm}$, $h = 12\,\mathrm{mm}$, $b = 28\,\mathrm{mm}$, and $D = 12\,\mathrm{mm}$.

It can be concluded from the results in Fig. 7 that if the input mass flow, $\dot{m}$, has a frequency component corresponding to the highest peak, it causes the pressure response to increase dramatically due to a resonant condition. Furthermore, it is also evident that the suction manifold is more or less sensitive to high amplitude gas pulsations at different operating speeds, which might be expected from Eq. (13) due to changes in the frequency spectrum of the single-cylinder mass flow profile, Q_{2n}. There is also something else about the pressure response that is not evident from Eq. (13) alone: the overall input–output frequency response of the pulsations actually changes with the spectrum of Q_{2n} due to the superposition (interactions) of the pressure responses attributable to the multiple valves in the manifold. In other words, the multiple input–output relationships from the various valves combine in different ways depending on the mass flow characteristics. This sensitivity to the source is rarely observed

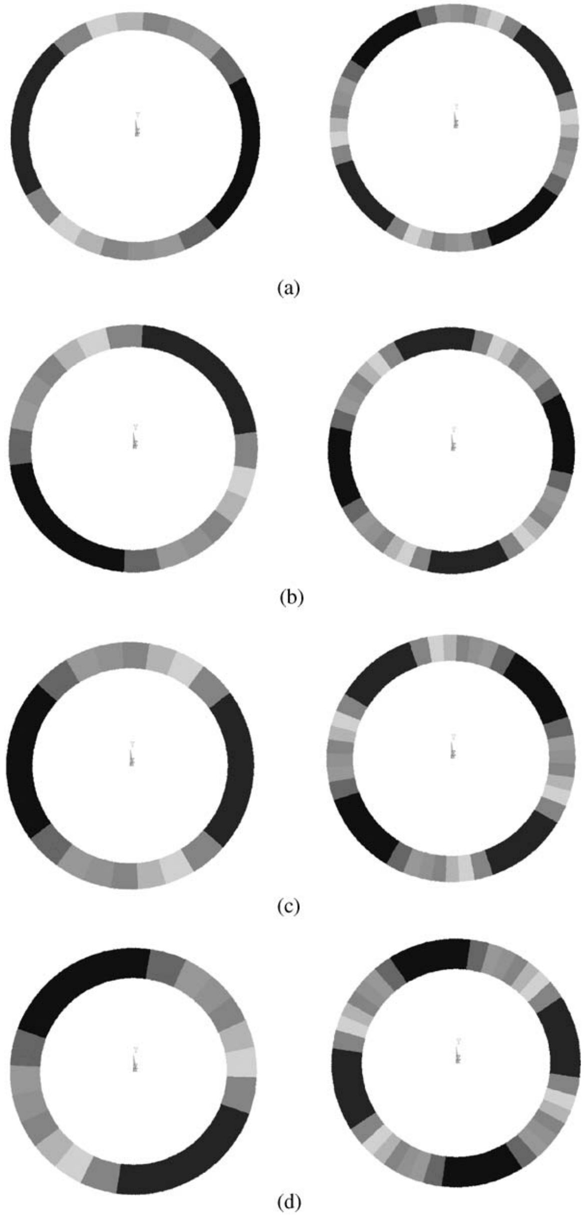

Fig. 5. First (left) and second (right) pressure mode shapes of the simplified suction manifold: (a) $h = 8\,\text{mm}$, (b) $h = 10\,\text{mm}$, (c) $h = 12\,\text{mm}$, and (d) $h = 14\,\text{mm}$.

in structural dynamic applications because there are not usually multiple phase-shifted but identical forces applied to a structure. This result demonstrates the importance of the nature of the mass flow rate time history, its corresponding frequency spectrum and the operating speed.

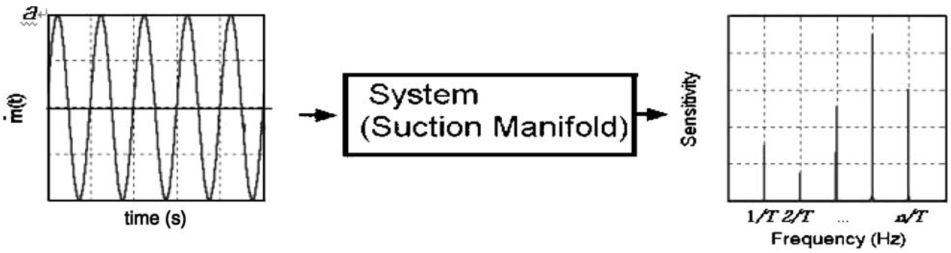

Fig. 6. Procedure for the calculation of the frequency response sensitivity.

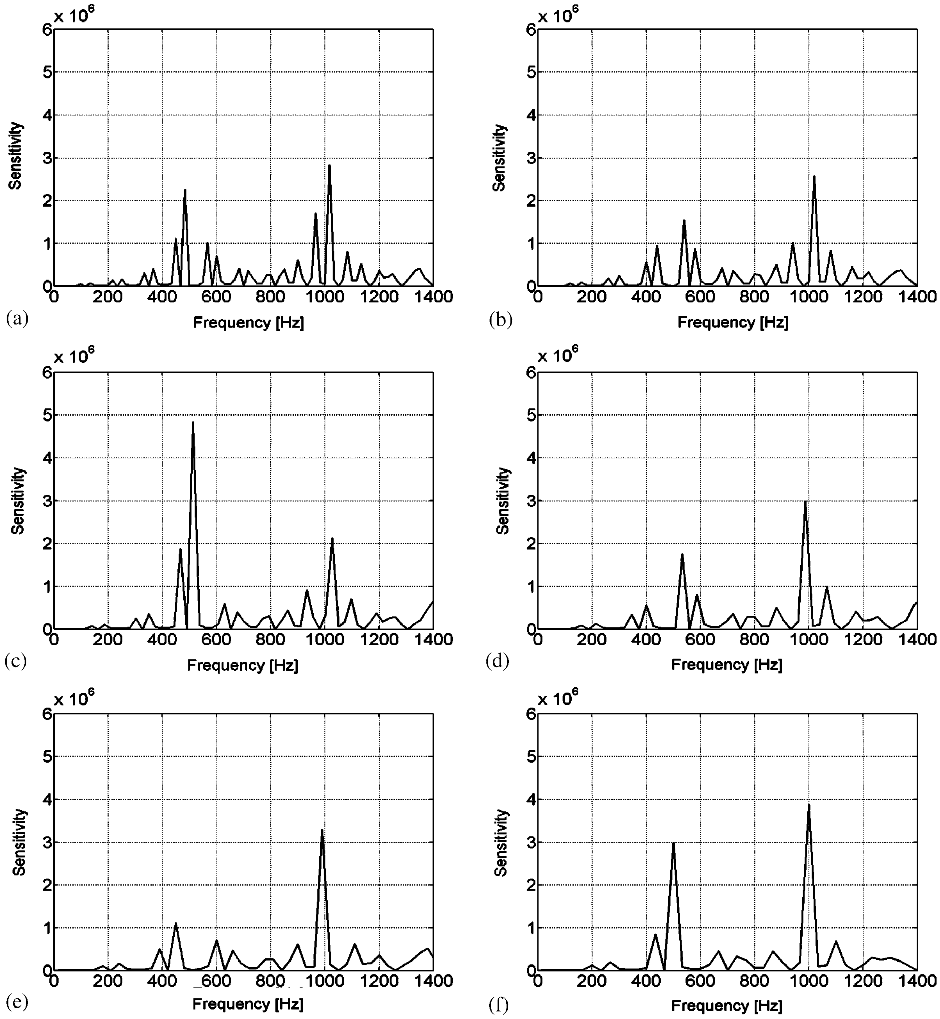

Fig. 7. Sensitivities as a function of frequency at: (a) 1000 r.p.m., (b) 1200 r.p.m., (c) 1400 r.p.m., (d) 1600 r.p.m., (e) 1800 r.p.m., and (f) 2000 r.p.m. of the compressor operating speeds.

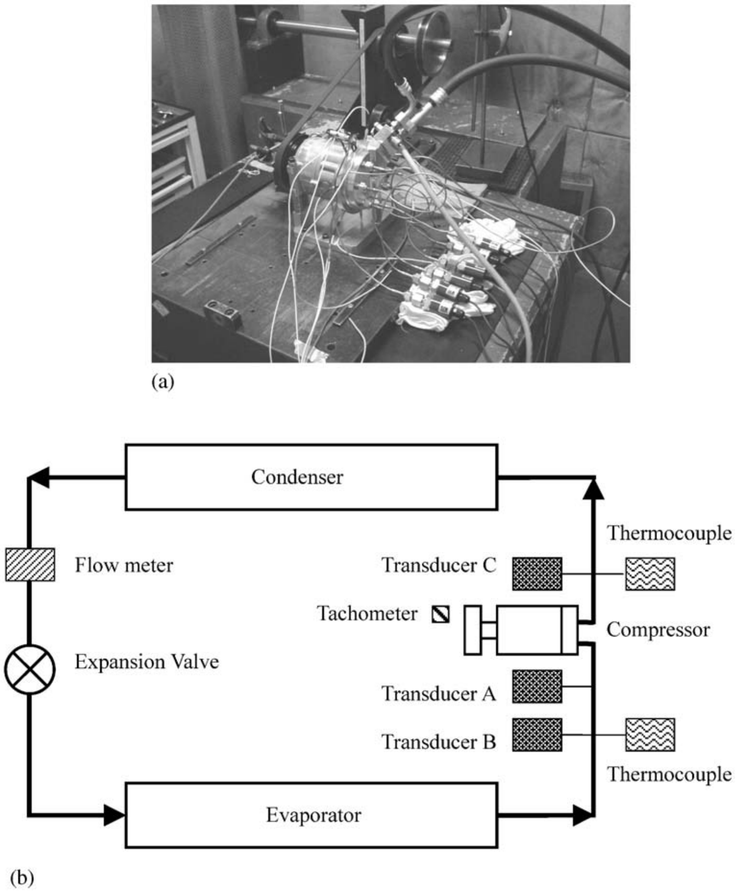

Fig. 8. (a) Compressor test stand for acquiring experimental dynamic pressure data and (b) schematic of experimental test apparatus.

2.3. Forced response experimental results

The purpose of this section is to introduce some representative experimental results by describing differences in the characteristics of pressure pulsations at various compressor operating speeds. This data was taken with the sophisticated compressor test stand setup pictured in Fig. 8(a) with the corresponding schematic diagram shown in Fig. 8(b). In order to measure the gas pulsation, seven valves operated at the same time with different phases. It has been noticed that in the compressor industry, it is difficult to control the anechoic termination [17,30]. Therefore, it has to be achieved by careful treatments. In order to eliminate the reflected wave and achieve the anechoic condition, a long suction pipe was used in the experiment. Measured variables in these experiments included operating speed, suction pulsation, static/mean suction pressure, suction gas temperature, and mean mass flow rate. Experimental results were selected at six different compressor operating speeds as listed in Table 3. The operating speed is seen to vary

Table 3
Operating conditions to investigate the effect of the compressor operating speed

Test	N_c (RPM)	P_d (MPa)	P_s (MPa)	T_d (°C)	T_s (°C)	Q (kg/h)	SH (°C)
1	1000	0.78	0.2110	57.4	15.0	90	13
10	1200	0.78	0.2110	58.3	15.0	90	13
19	1400	0.78	0.2060	57.0	12.3	90	11
28	1600	0.78	0.2010	60.4	14.6	90	14
37	1800	0.78	0.2060	58.6	14.0	90	13
46	2000	0.78	0.2060	61.6	15.0	90	14

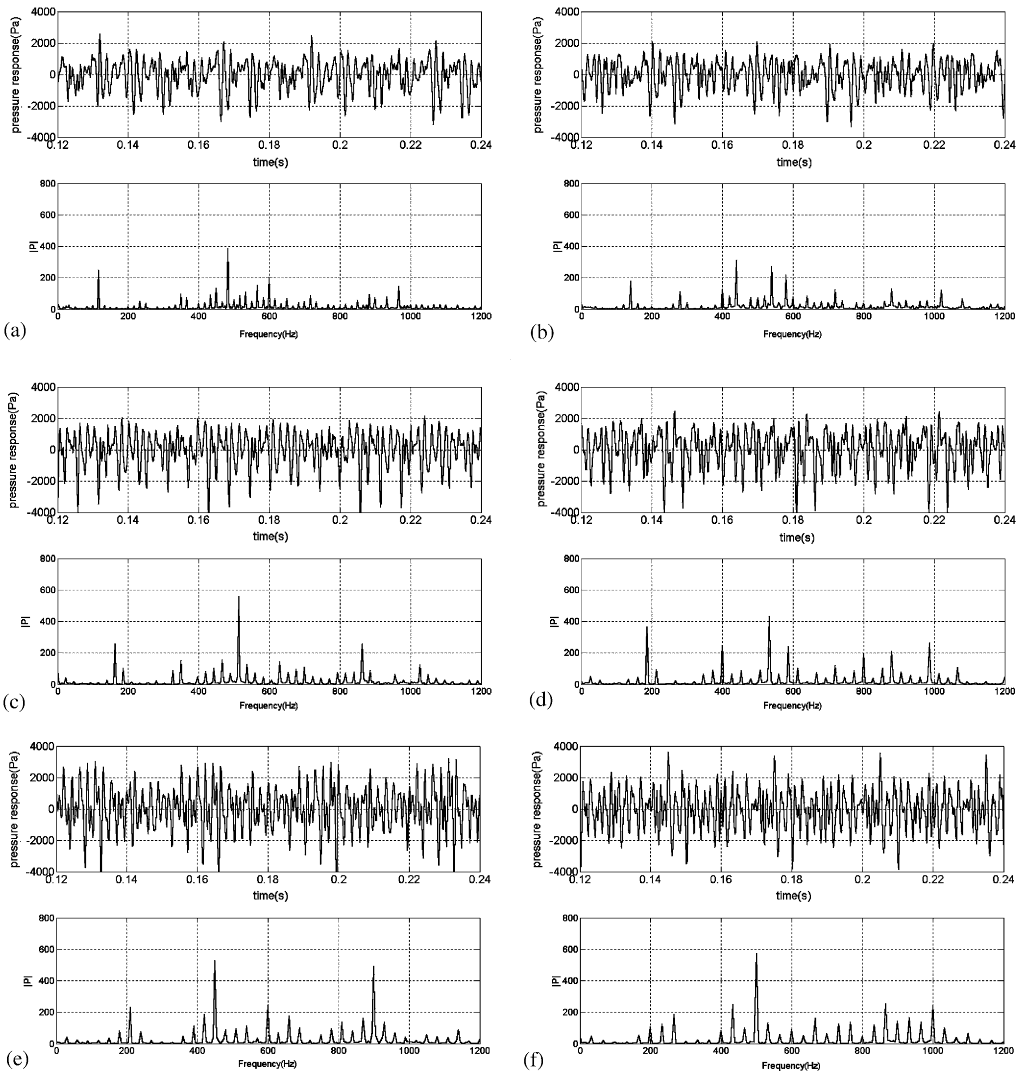

Fig. 9. Pressure pulsations in the time domain (upper) and frequency domain (lower) at: (a) 1000 r.p.m., (b) 1200 r.p.m., (c) 1400 r.p.m., (d) 1600 r.p.m., (e) 1800 r.p.m., and (f) 2000 r.p.m. of the compressor operating speeds.

from 1000 to 2000 r.p.m. The characteristics of the pressure pulsations are closely related to the operating speeds. As the operating speed increases, the pressure pulsations also increase. It should be noted that the highest peak of the pressure response in the frequency domain lies in the range of 400 and 600 Hz in Fig. 9, which shows the time and frequency spectra for the pressure data.

2.4. Source identification of pulsating flow sinks at valves

Although the idealized mass flow characteristic in Fig. 10 is analytically simple and can be computed directly from kinematic considerations, it is not an accurate portrayal of the true source at each valve port. In fact, when the ideal flow profile in Fig. 10 is applied to each of the valves, it fails to produce pressure pulsations at certain frequencies that are actually observed in the experimental data as shown in Figs. 15 and 17 (delay time = 0). In order to better represent the flow profile, the delayed valve opening time is included and an iterative approach is used to identify the actual flow source.

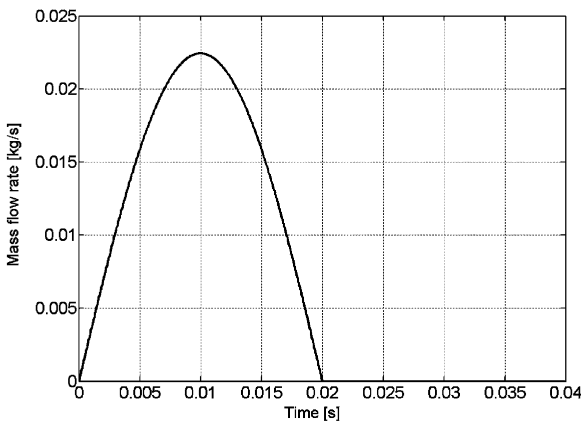

Fig. 10. Simple mass flow rate profile for 90 kg/h flow at 1500 r.p.m. speed for single valve.

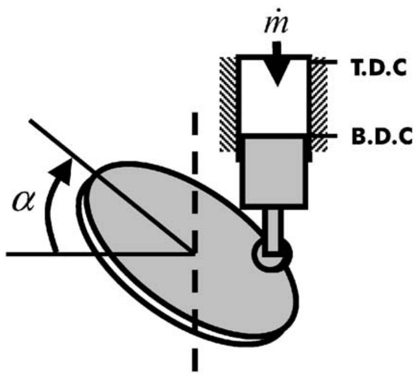

Fig. 11. Wobble swash plate cam.

As the swash plate turns on its axis, the range of the piston motion (Fig. 11) is determined by the operating conditions. Because the angle, α, of the swash plate varies with the operating conditions, the mass flow rate through the valve from the suction manifold can be determined by the motion of the piston. The velocity of the piston is governed by

$$\dot{h} = l_a \pi \frac{1}{60/n} \sin\left(2\pi \frac{1}{60/n} t\right), \tag{16}$$

where n is the operating speed (r.p.m) and l_a is the variable stroke of the piston, which is equal to the difference between the top dead center (TDC) and the lowest position of the piston for certain mass flow rate.

When the suction valves are open, the working compressor fluid passes from the suction manifold into the compressor cylinder. If the suction valve was not present, the gas flow would follow the velocity profile of the piston kinematics. But because of the interruption of the flow due to the valve, the gas flows into the cylinder from the suction manifold suddenly when the pressure in the cylinder reaches a certain level to open the valve. It is assumed that when the piston reaches the lowest position for certain mass flow rate, the valve closes immediately. The duration for opening the valve is expressed using a delay time, t_D, for opening the valve as shown in Fig. 12. In order to maintain a constant mass flow rate with the change in delay time, the variable stroke of the piston was calculated using the integration of the piston velocity as follows:

$$l_a = -\frac{M}{\rho} \frac{1}{N_v \times n \times 60} \frac{2}{A_1} \frac{1}{\cos\left(2\pi \frac{1}{60/n} \frac{T}{2}\right) - \cos\left(2\pi \frac{1}{60/n} t_D\right)}, \tag{17}$$

where M, N_v, A_1, T, ρ, n and t_D are the capacity of the mass flow rate, the number of the cylinder, cross-sectional area of the piston, the period, the density in the suction manifold, operating speed and the delay time for opening the valve, respectively.

Source identification is accomplished as follows: first, the parameters of the annular manifold are selected; second, the simple mass profile in Fig. 10 is applied and the forced response is simulated; third, the results of the simulation are compared with the experimental data and the

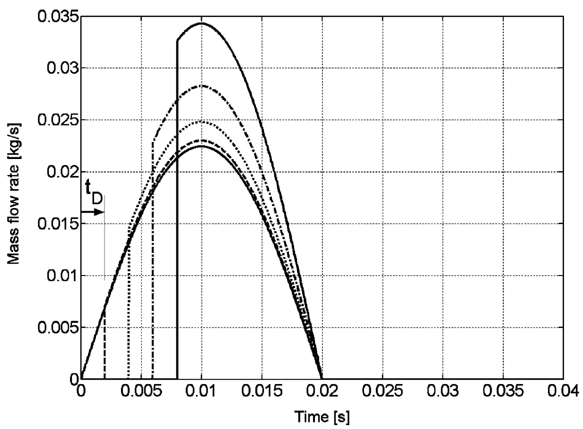

Fig. 12. Mass flow rate profiles for 90 kg/h flow at 1500 r.p.m. speed when the delayed time (t_D) is applied with the constant total mass flow rate (example: - - -, $t_D = 0.002$ s; $\cdots$, $t_D = 0.004$ s; $-\cdot-$, $t_D = 0.006$ s; —, $t_D = 0.008$ s).

(identical but phase shifted) flow sources at each valve are modified with an increase in the delay time for opening the valve (Fig. 12) to provide the same amplitude pulsation at 500 Hz as that observed in the experimental data; fourth, steps two and three are carried out iteratively until the simulation and test amplitudes match.

This 'inverse' procedure provides a more accurate mass flow rate estimate than the purely kinematic mass flow rate used previously. The overall objective here is to 'calibrate' the model assuming the differences between the experimental and analytical results are due solely to the source and not to any major dynamic misrepresentations (e.g., missing natural frequencies).

Using this approach, the variable stroke of the piston and the delay time for opening the valve are calculated without solving the valve dynamic and thermodynamic equations. The analytical results have a good agreement with the experimental results as shown in Fig. 13. But it is seen that the discrepancy of the results increases as the mass flow rate increases. From these results, the addition of the delay time for opening the valve is seen to be good for the low mass flow rate capacity. It can be concluded that the mass flow rate profile at 1500 r.p.m. with the 40 kg/h capacity (Fig. 14(a)) would capture the characteristic of the real mass flow rate very well.

The modified mass flow profile that is estimated from the frequency response of the experimental results at 1500 r.p.m. (fundamental frequency: 25 Hz) using the iterative procedure described above is shown at the right in Figs. 14 and 16 (40 kg/h capacity) and (90 kg/h capacity), respectively, with the corresponding discrete frequency spectrum in the left-hand-side plot. It is evident in the comparison between the idealized kinematic (dotted line) and modified (solid line) mass flows that there is a delay time for opening the valve that distorts the idealized profile.

The inclusion of the delayed time for opening the valve is also evident in the frequency spectrum, which clearly contains higher frequency components. These higher frequency components in the gas flow occur primarily because of the delay of the valve opening time.

The presence of the higher frequency components in the pulsating gas flow is important because even though their amplitudes are small near 484–500 Hz, these frequencies are dominant in determining the pressure response as is evident in the comparison between the experimental and simulation in Figs. 15 and 17. This high sensitivity in the frequency response characteristic of this

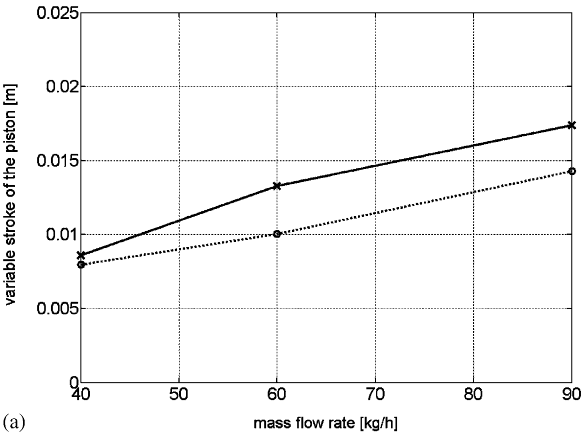

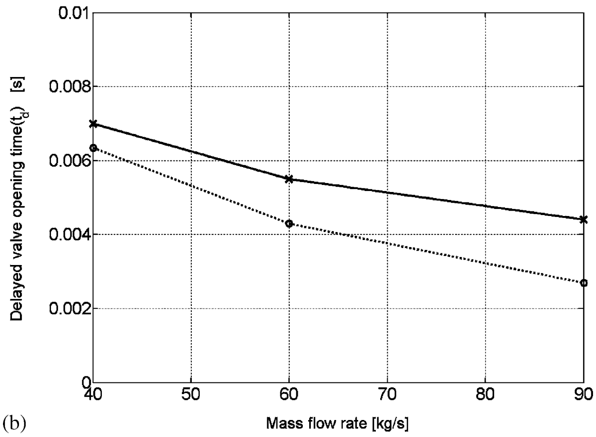

Fig. 13. Comparisons the experimental results of the estimated: (a) variable stroke of the piston for certain mass flow rate and (b) the delayed time for opening of the valve (-×-, experiment; ··○·· analysis).

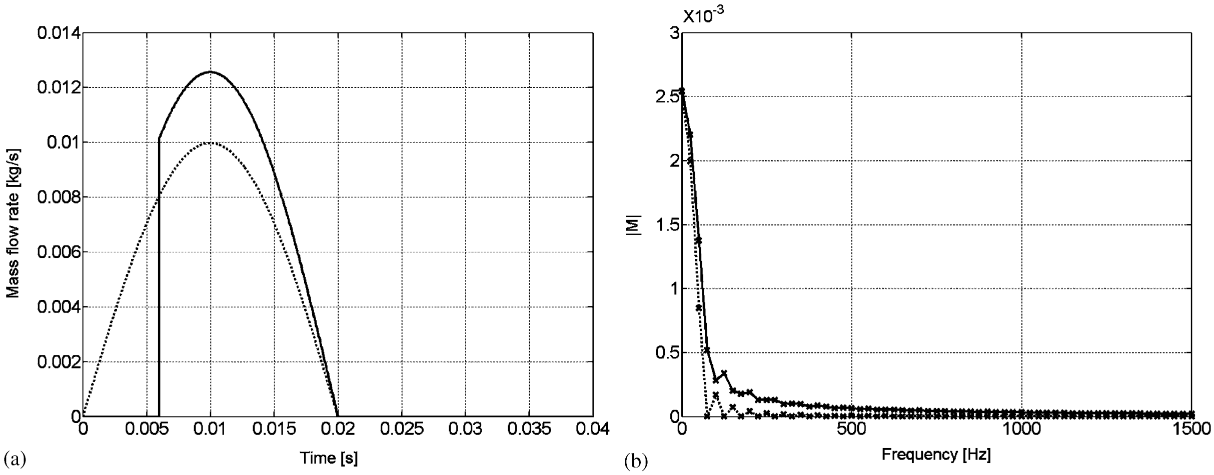

Fig. 14. Modified mass flow rate (—, $t_D = 0.0064\,\mathrm{s}$; $\cdots$, $t_D = 0\,\mathrm{s}$) in (a) the time domain and (b) the frequency domain for an operating speed of 1500 r.p.m. with a 40 kg/h capacity.

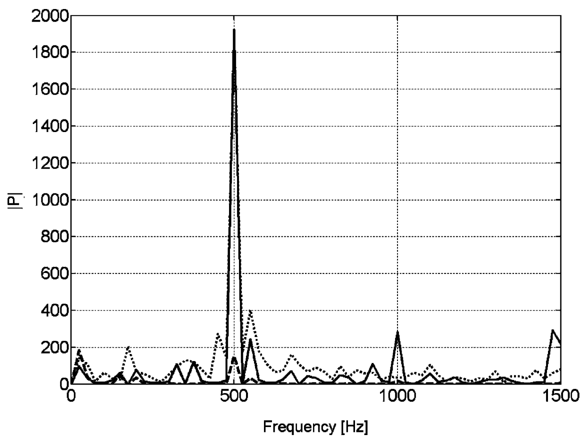

Fig. 15. Pressure responses in the frequency domain using the modified mass flow rate with comparison between simulation (—, $t_D = 0.0064\,\mathrm{s}$; - - - -, $t_D = 0\,\mathrm{s}$) and test ($\cdots$) results.

multi-source/sink single output system was explained above in Section 2.2 by analyzing the change in sensitivity with operating speed. Note in the figure that the agreement for the 40 kg/h capacity (Fig. 15) is very good; however, at the higher mass flow rate, the error in the estimated pressure pulsation (Fig. 17) is larger.

The modified mass flow profile that was estimated from the frequency response of the experimental results at 1500 r.p.m. with a 90 kg/h capacity (Fig. 18(b)) using the iterative procedure described above is shown in Fig. 18(a). It is evident in the comparison between the idealized kinematic (dashed line) and modified (solid line) mass flows that there is a large modulating frequency component that distorts the idealized profile. The 'inverse' procedure

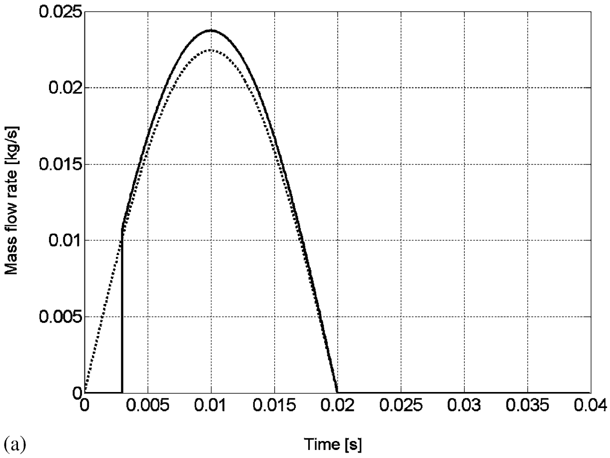

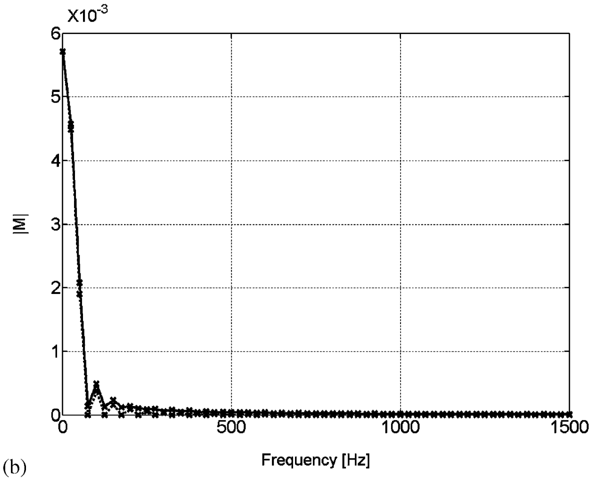

Fig. 16. Modified mass flow rate (—, $t_D = 0.0027$ s; $\cdots$, $t_D = 0$ s) in (a) the time domain and (b) the frequency domain for an operating speed of 1500 r.p.m. with a 90 kg/h capacity.

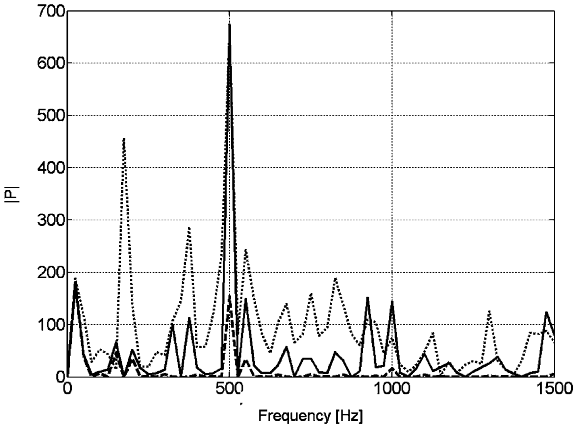

Fig. 17. Pressure responses in the frequency domain using the mass flow rate including the delayed time with comparison between simulation (—, $t_D = 0.0027$ s; - - - -, $t_D = 0$ s) and test ($\cdots$) results.

provides a more accurate mass flow rate estimate than the purely kinematic mass flow rate and the simple inclusion of the delay time used previously. From the results, it is clear that a good estimate of the pressure pulsations is only possible when a good estimate of the mass flow rate source is available including even its most subtle harmonic components. The variable stroke of the piston and the delay time can be accurately estimated by comparing the gas pulsations from the experiments with those from the forced response simulations. Note that the estimation of the gas pulsation is more accurate for low mass flow rates. It is thought that the inaccuracy at the higher frequency is due to the interaction of the valve, turbulent flow and so on.

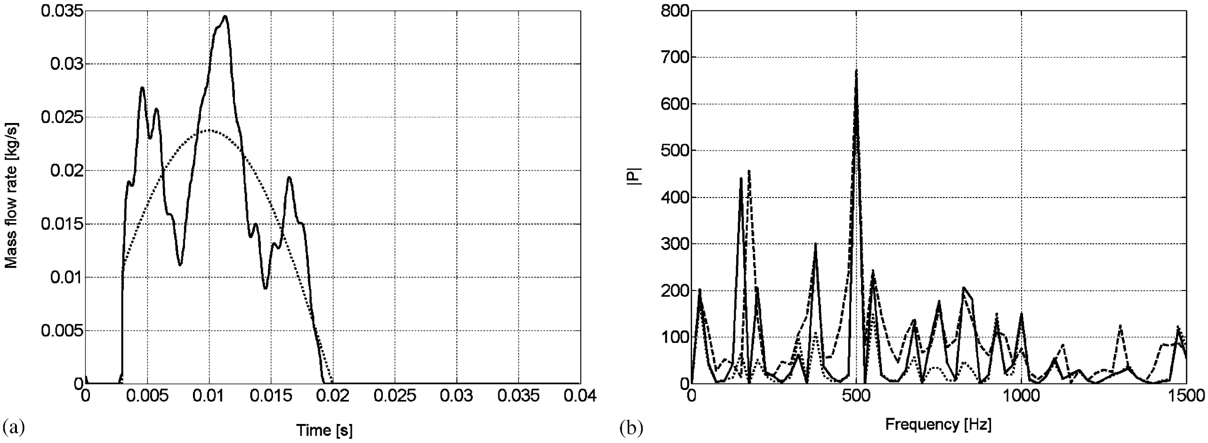

Fig. 18. (a) Modified mass flow rate and (b) pressure responses in the frequency domain using the modified mass flow rate with comparison between simulation ($\cdots$, $t_D = 0.0027\,\mathrm{s}$; —, $t_D = 0.0027\,\mathrm{s}$ and iterative procedure) and test (- - - -) results for an operating speed of 1500 r.p.m. with a 90 kg/h capacity.

3. Conclusions

A complicated suction manifold geometry is modelled as a simplified cylindrical annular cavity using finite element analysis to select the mean radius of the manifold to dynamically match the frequency spectrum of the actual manifold. It is demonstrated that complicated interactions between multiple cylinders in a suction manifold can produce unexpected changes in the frequency response resonant conditions for changes in the frequency content of the source flow rates due to changes in operating speed. These changes in the frequency response are not due to changes in resonant frequencies since the mean radius was fixed, but were instead due to the superposition of multiple inlet-valve pairs. It is also shown that the delay time for opening the valve and variable stroke of the piston can be estimated without solving the valve dynamic and thermodynamic equations. Using the delay time, the estimate of the gas pulsation in the suction manifold, which were subsequently identified using an iterative procedure in conjunction with the modal expansion simulation procedure, is in good agreement with the experimental result in the case of lower mass flow capacity. By using the source mass flow rates as identified at 1500 r.p.m. with a 90 kg/h capacity, the correlation between analytical and experimental results was shown to be much better than if the idealized source functions were used instead.

References

[1] E.U. Condon, H. Odishaw, *Handbook of Physics*, McGraw-Hill, New York, 1958.
[2] P.E. Doak, Analysis of internally generated sound in continuous materials: (I) inhomogeneous acoustic wave equations, *Journal of Sound and Vibration* 2 (1965) 53–73.
[3] P.A. Franken, Generation of sound in cavities by flow rate change, *Journal of the Acoustical Society of America* 33 (1961) 1193–1195.
[4] A. Cummings, Sound transmission in curved duct bends, *Journal of Sound and Vibration* 35 (1974) 451–477.
[5] P.B. Subrahmanyam, R.I. Sujith, T.C. Lieuwen, A family of exact transient solutions for acoustic wave propagation in inhomogeneous, non-uniform area ducts, *Journal of Sound and Vibration* 240 (2001) 705–715.

[6] P.C.C. Lai, W. Soedel, Two dimensional analysis of thin, shell or plate like muffler elements, *Journal of Sound and Vibration* 194 (1996) 137–171.
[7] P.C.C. Lai, W. Soedel, Two dimensional analysis of thin, shell or plate like muffler elements of non-uniform thickness, *Journal of Sound and Vibration* 195 (1996) 445–475.
[8] P.C.C. Lai, W. Soedel, Free gas pulsations in acoustic systems composed of two thin, curved or flat, two-dimensional gas cavities which share a common open boundary, *Journal of Sound and Vibration* 198 (1996) 225–248.
[9] J. Kim, W. Soedel, Development of a general procedure to formulate four pole parameters by modal expansion and its application to three dimensional cavities, *Transactions of the American Society of Mechanical Engineers* 112 (1990) 452–459.
[10] J. Kim, W. Soedel, General formulation of four pole parameters for three dimensional cavities utilizing modal expansion with special attention to the annular cylinder, *Journal of Sound and Vibration* 129 (1989) 237–254.
[11] J. Kim, W. Soedel, Analysis of gas pulsations in multiply connected three dimensional acoustic cavities with special attention to natural mode or wave cancellation effects, *Journal of Sound and Vibration* 131 (1989) 103–114.
[12] C.H. Kung, R. Singh, Experimental modal analysis technique for three dimensional acoustic cavities, *Journal of the Acoustical Society of America* 77 (1985) 731–738.
[13] F. Pan, J.D. Jones, Gas path sound transmission in spherically shaped reciprocating compressors: theory and experiment, *Transactions of the American Society of Mechanical Engineers* 121 (1999) 8–17.
[14] J.C. Snowdon, Mechanical four pole parameters and their application, *Journal of Sound and Vibration* 15 (1971) 307–323.
[15] P.C.C. Lai, W. Soedel, Gas pulsations in thin, curved or flat cavities due to multiple mass flow sources, *Proceedings of International Compressor Engineering Conference*, Purdue, 1996, pp. 799–805.
[16] S. Sun, T. Ren, New method of thermodynamic computation for a reciprocating compressor: computer simulation of working process, *International Journal of Mechanical Science* 37 (1995) 343–353.
[17] P.C.C. Lai, A study of the acoustical termination on practical gas pulsation measurement, *Journal of Sound and Vibration* 233 (2000) 617–641.
[18] J.P. Elson, W. Soedel, Simulation of the interaction of compressor valves with acoustic back pressures in long discharge lines, *Journal of Sound and Vibration* 34 (1974) 211–220.
[19] J. Kim, W. Soedel, Four pole parameters of shell cavity and application to gas pulsation modeling, *Proceedings of International Compressor Engineering Conference*, Purdue, 1988, pp. 331–337.
[20] J.F. Hamilton, D.D. Schewerzler, simulation and design studies of a multiple cylinder refrigeration compressor, *Proceedings of International Compressor Engineering Conference*, Purdue, 1972, pp. 5–12.
[21] W. Soedel, J.M. Baum, natural frequencies and modes of gases in multi-cylinder compressor manifolds and their use in design, *Proceedings of International Compressor Engineering Conference*, Purdue, 1976, pp. 257–270.
[22] P.C.C. Lai, W. Soedel, D. Gilliam, P. Roy, On the permissibility of approximating irregular cavity geometries by reciprocating boxes and cylinders, *Proceedings of International Compressor Engineering Conference*, Purdue, 1996, pp. 807–813.
[23] R. Singh, W. Soedel, Mathematical modeling of multicylinder compressor discharge system interactions, *Journal of Sound and Vibration* 63 (1979) 125–143.
[24] Z. Zhou, J.F. Hamilton, Multicylinder reciprocating refrigerating compressor modeling, *Proceedings of International Compressor Engineering Conference*, Purdue, 1986, pp. 669–683.
[25] J. Kim, Application of four pole parameters for gas pulsation analysis of multi-cylinder compressors with symmetrical arranged gas cavities, *Proceedings of International Compressor Engineering Conference*, Purdue, 1992, pp. 1487–1494.
[26] P.C.C. Lai, W. Soedel, Gas pulsation in thin, curved or flat cavities due to multiple mass flow sources with special attention to multi-cylinder compressors, *Journal of Sound and Vibration* 197 (1996) 45–66.
[27] W. Soedel, Gas Pulsations in Compressor and Engine Manifold, Short Course Text Book, Purdue University, 1978.
[28] W. Soedel, *Vibrations of Shells and Plates*, Marcel Dekker, New York, 1993.
[29] W. Zhou, J. Kim, Formulation of four poles of three-dimensional acoustic systems from pressure response functions with special attention to source modeling, *Journal of Sound and Vibration* 219 (1999) 89–103.
[30] M.L. Munjal, An error inherent in the use of the two-microphone method for gas pulsation measurement in a reflective environment, *Journal of Sound and Vibraion* 242 (2001) 539–541.